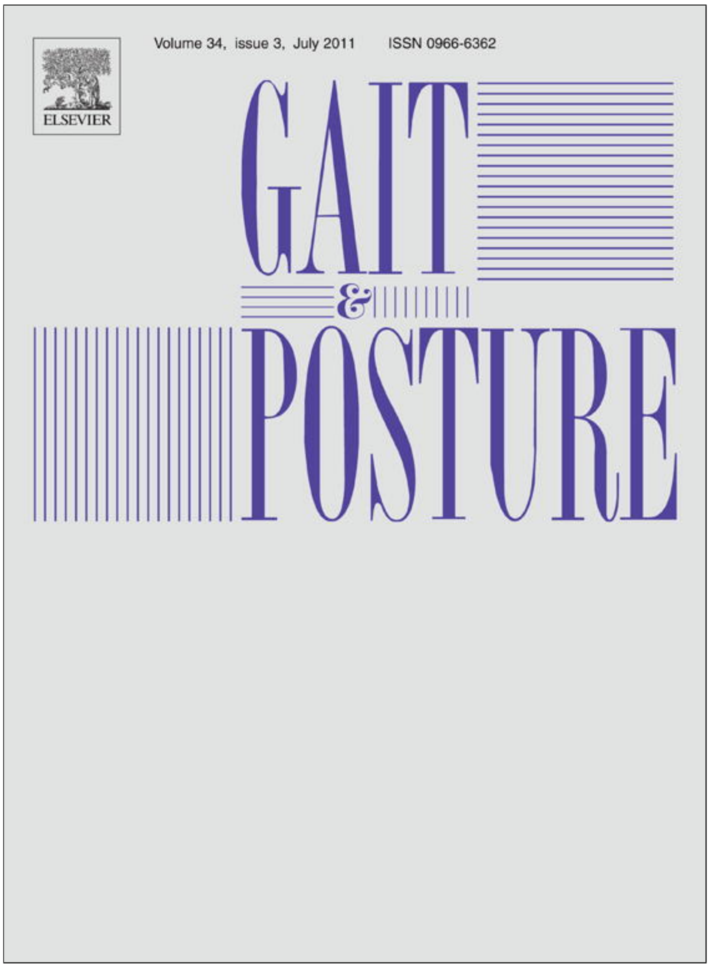
Volume 34, issue 3, July 2011
ISSN 0966-6362
ELSEVIER
GAIT
&
POSTURE

Gait & Posture 34 (2011) 320–323

Contents lists available at ScienceDirect

Gait & Posture

journal homepage: www.elsevier.com/locate/gaitpost

# Quantification of inertial sensor-based 3D joint angle measurement accuracy using an instrumented gimbal

A. Brennan [a], J. Zhang [a], K. Deluzio [a,b], Q. Li [a,b,*]

[a] Department of Mechanical and Materials Engineering, Queen's University, Kingston, ON, Canada
[b] Human Mobility Research Centre, Queen's University and Kingston General Hospital, Kingston, ON, Canada

ARTICLE INFO

*Article history:*
Received 7 September 2010
Received in revised form 27 January 2011
Accepted 23 May 2011

*Keywords:*
3D knee kinematics
Joint coordinate system
Instrumented gimbal
Inertial sensor accuracy
Knee joint angles

ABSRACT

This study quantified the accuracy of inertial sensors in 3D anatomical joint angle measurement with respect to an instrumented gimbal. The gimbal rotated about three axes and directly measured the angles in the ISB recommended knee joint coordinate system. Through the use of sensor attachment devices physically fixed to the gimbal, the joint angle estimation error due to sensor attachment (the inaccuracy of the sensor attachment matrix) was essentially eliminated, leaving only error due to the inertial sensors. The angle estimation error (RMSE) corresponding to the sensor was found to be 3.20° in flexion/extension, 3.42° in abduction/adduction and 2.88° in internal/external rotation. Bland–Altman means of maximum absolute value were −1.63° inflexion/extension, 3.22° in abduction/adduction and −2.61° in internal/external rotation. The magnitude of the errors reported in this study imply that even under ideal conditions irreproducible in human gait studies, inertial angle measurement will be subject to errors of a few degrees. Conversely, the reported errors are smaller than those reported previously in human gait studies, which suggest that the sensor attachment is also significant source of error in inertial gait measurement. The proposed apparatus and methodology could be used to quantify the performance of different sensor systems and orientation estimation algorithms, and to verify experimental protocols before human experimentation.



## 1. Introduction

Quantification of knee joint kinematics is important in the diagnosis of knee joint disorders, in the evaluation of functional ability following rehabilitation [1], and in the control of wearable robotic devices [2]. Motion capture systems are capable of quantifying knee joint kinematics with a high accuracy. However they are expensive, sophisticated, and require a dedicated laboratory, all of which limit their usage. To bring the analysis out of the laboratory and make it portable, recent efforts have focused on estimating knee joint kinematics using accelerometers and gyroscopes. The combination of these sensors is referred to as an inertial measurement unit (IMU). Most studies using accelerometers and gyroscopes have been limited to only estimating 2D knee joint angles, flexion/extension [3–8]. Some studies [9] and [10] have used pendulum devices to quantify the accuracy of IMU based sensors in planar motion. Although the results reflect the sensor performance for 2D motion, they may not accurately extrapolate the performance into 3D motion.

Recently, proposed a novel IMU alignment procedure and calculated the 3D knee joint angle as the relative angle between the thigh and shank segments [11]. By implementing a new passive movement-based functional calibration procedure [11] and [12], extended their earlier work [11] to estimate anatomical knee joint angle according to the International Society of Biomechanics (ISB) recommendation [13]. Although the proposed IMU system showed good precision when compared with a magnetic marker-based reference system, the accuracy in knee joint angle estimation was limited (between 4.0° and 8.1°). Because IMU based and magnetic based systems both estimate anatomical knee joint angles indirectly, it was methodologically impossible to isolate the sources of error in the knee joint angle estimates. This led to the inability to draw a definitive conclusion on the performance of inertial sensors in estimating 3D knee joint angles. To determine the feasibility of using inertial sensors in estimating 3D angles, it is necessary to quantify the performance of an IMU system by comparing the anatomical joint angle estimates with those directly measured from a device with a higher accuracy. We have built an instrumented gimbal to be an accurate reference system for quantifying 3D IMU error. Furthermore, because the gimbal has fixed attachment sites in known positions, the discrepancy between the gimbal and the IMU joint angles is dominated by 3D angle estimation error of the IMU.

* Corresponding author at: Department of Mechanical & Materials Engineering, Queen's University 130 Stuart St., Kingston, Canada. Tel.: +1 613 533 3191.
*E-mail address:* qli@me.queensu.ca (Q. Li).

0966-6362/$ – see front matter. Crown Copyright © 2011 Published by Elsevier B.V. All rights reserved.
doi:10.1016/j.gaitpost.2011.05.018

## 2. Materials and methods

### 2.1. Instrumented gimbal

The gimbal is a right knee model that consists of two rigid segments, named the femur and tibia, which rotate about 3 axes that intersect at a center of rotation. One axis of rotation ($\vec{i}$) is lateral to the femur segment, corresponding to knee flexion/extension. Another axis ($\vec{k}$) is aligned axially with the tibia segment, corresponding to knee internal/external rotation; the third axis ($\vec{j}$) is defined to be perpendicular to the plane formed by the other two axes ($\vec{k}\times\vec{i}$), corresponding to adduction/abduction (Fig. 1). As recommended by ISB [14], the sequence of rotations ($\vec{i}-\vec{j}-\vec{k}$) defines the knee angles in the Joint Coordinate System (JCS) with $\alpha_g$ for flexion/extension of the gimbal, $\beta_g$ for abduction/adduction, and $\gamma_g$ for internal/external rotation. These angles, measured directly by a potentiometer attached to the bearing of each axis, were used to quantify performance of the IMU system in estimating 3D anatomical joint angle. In this study, two IMUs (sensor model: Inertia-Link by Microstrain Inc., VT.) were attached to the gimbal, one to the femur segment and the other to the tibia limb segment via mounting brackets (Fig. 1). The IMU mounting brackets were designed to ensure proper alignment of the sensor axes with the gimbal axes (Figs. 1 and 2). The gimbal is activated by manually moving the femur.

### 2.2. Anatomical joint angles measured by IMUs

The definitions of individual frames and sequences of transformations for computing 3D joint angles are illustrated in Fig. 2. Each IMU (ADXL accelerometer, $\pm$5 g; ADXRS gyroscope, $\pm 600^\circ$/s) is equipped with a proprietary orientation algorithm that estimates segment orientation with high accuracy ($\pm 0.5^\circ$ static and $\pm 2^\circ$ dynamic; as per product specifications). The sensors produce an orientation matrix, $M$, based on algorithms embedding in the on-board hardware. The form of the orientation matrix, $M$, can be found in the DCP (Data-Communications Protocol) manual for the sensors. A basic explanation of how the angle is measured by the sensors is provided in the paper by [15]. The orientation matrix $M$ transfers a vector, $V_E$, in the earth frame into a vector in the local measurement frame, $V_L$, as follows:

$$V_L = MV_E. \tag{1}$$

While the $X$ and $Y$ axes of the earth frames of two IMUs generally do not coincide with each other, the vertical $Z$ axes are assumed to be equal [11]. To align the $X$ and $Y$ axes, we followed a modified version of the procedure proposed by [11], which incorporates an additional hip flexion/extension motion in the alignment procedure. This determined the earth frame alignment matrix $S$ (Fig. 2), parameterized by the earth frame alignment angle $\theta$. However, we observed that the earth frame alignment angle $\theta$ is not stationary. Therefore, instead of a single calibration [11], we performed

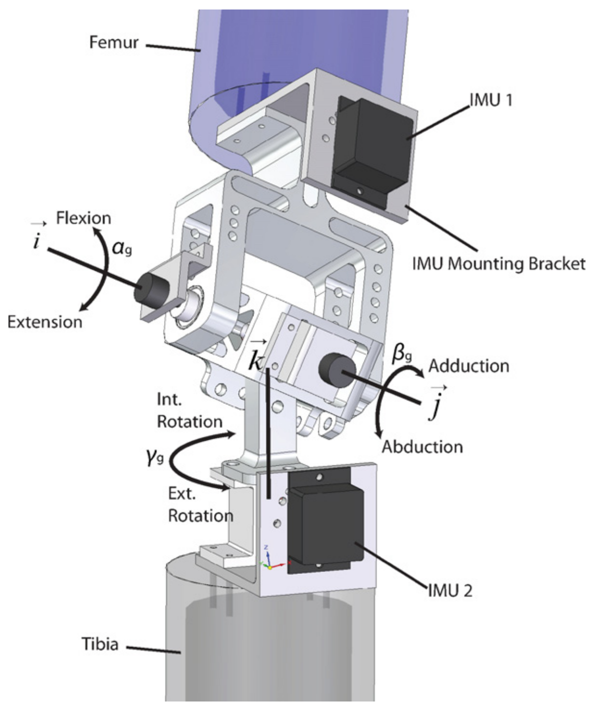


**Fig. 1.** Proposed testing apparatus: the instrumented gimbal. IMU sensor location and mounting brackets are defined in this frontal view of the right knee, along with axis definitions, rotation directions, and angle association. The angle association is given for movement of the femur with a fixed tibia, as that is the motion that was performed.

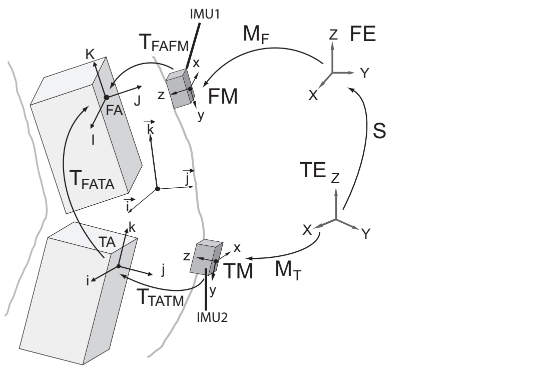


**Fig. 2.** Individual frames and the sequence of transformation for knee anatomical angle estimation. *TA* and *FA* define the anatomical frames for tibia and femur respectively. The sensor measurement frames for tibia and femur are denoted *TM* and *FM*. Time-invariant sensor attachment matrices, $T_{TATM}$ and $T_{FAFM}$, transform a vector in the sensor measurement frames to the anatomical frames. The time-dependent orientation matrices, $M_T$ and $M_F$, describes the orientations of the tibia and femur with respect to their corresponding earth frame, *TE* and *FE* respectively. The *z* axes of the earth frames are aligned, but the *x–y* coordinates are distinct from each other. The alignment between these two earth frames can be represented by a rotation matrix $S$ with a rotation of angle $\theta$ about the gravitational $z$-axis [12].

the earth frame alignment procedure before and after data collection to compensate for the effect of drift on earth frame alignment. With the earth frame alignment angle $\theta_1(t_1)$ prior to data collection and $\theta_2(t_2)$ after data collection, the earth frame alignment angle during the experiment at time $t$ is approximated by

$$\theta(t) = \frac{\theta_2-\theta_1}{t_2-t_1}(t-t_1), \tag{2}$$

Anatomical angles are considered as an $i$–$j$–$k$ Cardan/Euler rotation from a fixed femur anatomical (FA) frame to a moving tibia anatomical (TA) frame. The corresponding rotation matrix $T_{FATA}$ is calculated as the following product:

$$T_{FATA} = T_{FAFM} M_F S M_T^{-1} T_{TATM}^{-1}, \tag{3}$$

where $T_{TATM}$ and $T_{FAFM}$ are sensor attachment matrices, which are time-invariant transformation matrices between measurement and anatomical frames, and $S$ aligns the femur and tibia coordinate frames according to the angle $\theta$. The time-dependent orientation matrices, $M_T$ and $M_F$, describe the orientations of the tibia and femur with respect to their corresponding earth frames, *TE* and *FE* respectively (Fig. 2).

From Eq. (3), there are three potential sources that contribute to 3D angle estimation error: sensor attachment matrices ($T_{FAFM}$ and $T_{TATM}$), sensor orientation matrices ($M_F$ and $M_T$), and the earth frame alignment matrix ($S$). The latter two sources of error are directly related to the inertia sensors, and the first source of error is attributed to sensor attachment inaccuracy caused by the user. To isolate the sensor accuracy, we eliminated the first source by using IMU mounting brackets on the gimbal. The IMU mounting brackets were designed to produce the sensor attachment matrices, $T_{FAFM}$ and $T_{TATM}$, as

$$T_{FAFM} = T_{TATM} = \begin{bmatrix} -1 & 0 & 0 \\ 0 & 0 & -1 \\ 0 & -1 & 0 \end{bmatrix}. \tag{4}$$

The relationship between anatomical angles and the Cardan rotation matrix is given by:

$$T_{FATA} = \begin{bmatrix} \cos\beta\cos\gamma & -\sin\gamma\cos\beta & \sin\beta \\ \cos\gamma\sin\beta\sin\alpha+\sin\gamma\cos\alpha & \cos\alpha\cos\gamma-\sin\alpha\sin\beta\sin\gamma & -\cos\beta\sin\alpha \\ \sin\gamma\sin\alpha-\cos\gamma\sin\beta\cos\alpha & \sin\gamma\sin\beta\cos\alpha+\cos\gamma\sin\alpha & \cos\beta\cos\alpha \end{bmatrix}, \tag{5}$$

and the angles were calculated as

$$\begin{aligned} \beta &= \sin^{-1}(T_{FATA}(1,3)) \\ \alpha &= \tan_2^{-1}\left(\frac{-T_{FATA}(2,3)}{T_{FATA}(3,3)}\right) \\ \gamma &= \tan_2^{-1}\left(\frac{-T_{FATA}(1,2)}{T_{FATA}(1,1)}\right). \end{aligned} \tag{6}$$

where $\tan^2_{-1}$ is the four quadrant arctangent.

### 2.3. Experiment and data analysis

The IMUs were securely attached to the mounting brackets on the gimbal to achieve the sensor attachment matrix of Eq. (4) (Fig. 2). The reference angles

**Table 1**
Sensor error results in RMSE and Bland–Altman.

| Trial # | Drift | Max angular rate | Anatomical angle | RMSE (% error ROM) | Bland–Altman mean (SD) | Limits of agreement |
|---|---|---|---|---|---|---|
| 1 | −0.010°/s | 175.23°/s | Flex/Ext | 2.97 (1.89%) | −1.63 (2.49) | (−6.61, 3.34) |
| | | | Add/Abd | 2.00 (3.41%) | 0.98 (1.74) | (−2.50, 4.47) |
| | | | Int/Ext rotation | 1.59 (1.55%) | −0.29 (1.56) | (−3.42, 2.84) |
| 2 | −0.006°/s | 198.98°/s | Flex/Ext | 2.18 (1.58%) | −1.41 (1.66) | (−4.72, 1.90) |
| | | | Add/Abd | 3.42 (5.64%) | 3.22 (1.16) | (0.89, 5.54) |
| | | | Int/Ext rotation | 1.91 (1.76%) | −1.47 (1.21) | (−3.90, 0.96) |
| 3 | 0.017°/s | 210.60°/s | Flex/Ext | 3.20 (1.71%) | −0.11 (3.19) | (−6.50, 6.28) |
| | | | Add/Abd | 2.12 (3.48%) | 0.88 (1.93) | (−2.98, 4.73) |
| | | | Int/Ext rotation | 2.37 (2.45%) | 0.39 (2.34) | (−4.29, 5.07) |
| 4 | 0.011°/s | 199.07°/s | Flex/Ext | 2.58 (1.66%) | −1.57 (2.04) | (−5.66, 2.51) |
| | | | Add/Abd | 1.47 (2.89%) | 0.36 (1.43) | (−2.50, 3.21) |
| | | | Int/Ext rotation | 2.88 (2.41%) | −2.61 (1.21) | (−5.02, −0.20) |
| 5 | -0.004°/s | 232.98°/s | Flex/Ext | 2.94 (1.63%) | −1.19 (2.69) | (−6.56, 4.19) |
| | | | Add/Abd | 1.94 (3.19%) | 0.24 (1.92) | (−3.60, 4.08) |
| | | | Int/Ext rotation | 1.28 (0.85%) | −0.08 (1.28) | (−2.64, 2.48) |

measured by the potentiometers and the IMU orientation recordings were taken at a rate of 100 Hz and synchronized using a customized program to start and stop both systems simultaneously.

We performed five independent trials where data collection was taken for 2 min for a sequence of random motion. Although the motion sequence was completely randomized and performed manually, a visual attempt was made to maintain angular velocity below the maximum angular velocity experienced during flexion/extension in normal gait. For the data collection, one IMU was attached to each segment of the gimbal. The earth frame alignment calibration process was followed as described in Section 2.2, for which both sensors were attached to the upper segment of the gimbal. The gimbal is capable of locking internal/external rotation such that only abduction/adduction and flexion/extension motion are possible for the calibration procedure.

Agreement of the joint angle waveforms between the reference gimbal and the inertial method was quantified in two ways: using the root mean square error (RMSE) as per Eq. (7), and using the Bland–Altman limits of agreement [16]. The Bland–Altman method provides an interval within which the angle estimation errors fall with a 95% probability. All the data analysis was carried out in MATLAB (Mathworks Inc. Natick, MA).

$$\begin{aligned} \mathrm{RMSE}(\alpha) &= \sqrt{\frac{\sum_{n=1}^{N}(\alpha(n)-\alpha_g(n))^2}{N}} \\ \mathrm{RMSE}(\beta) &= \sqrt{\frac{\sum_{n=1}^{N}(\beta(n)-\beta_g(n))^2}{N}} \\ \mathrm{RMSE}(\gamma) &= \sqrt{\frac{\sum_{n=1}^{N}(\gamma(n)-\gamma_g(n))^2}{N}} \end{aligned} \quad (7)$$

where $N$ is the number of samples in a trial.

## 3. Results

The results are summarized in Table 1 with RMSE, relative error (%) to the total range of motion, and Bland–Altman measures. The corresponding earth frame drift rate and the maximum angular velocity for each trial are also provided in the table.

Although variability exists between trials, the errors exhibit similar means and limits of agreement. The maximum RMSE values observed were 3.20° in flexion/extension (trial three), 3.42° in abduction/adduction (trial two) and 2.88° in internal/external rotation (trial four). The mean RMSE with standard deviation is: 2.77° (0.40°) in flexion/extension, 2.19° (0.73°)in abduction/adduction, and 2.01° (0.63°) in internal/external rotation.

The Bland–Atlman method provides an interval within which the angle estimation errors fall with a 95% probability (2 × standard deviation), which is shown as the right-most column of Table 1. Bland–Altman means of maximum absolute value were −1.63° in flexion/extension (trial one), 3.22° in abduction/adduction (trial two) and −2.61° in internal/external rotation (trial four). A representative plot is shown in Fig. 3, which

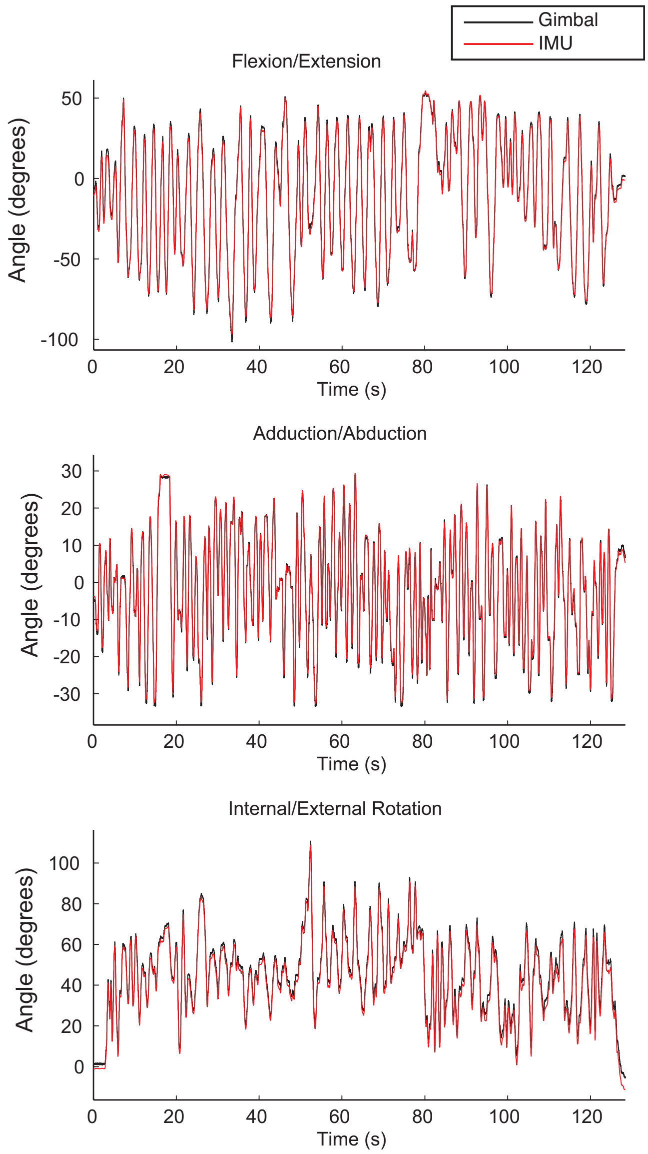


**Fig. 3.** Representative joint angle estimation results from inertial measurement (in red) and the gimbal (in black). (For interpretation of the references to color in this figure legend, the reader is referred to the web version of the article.)

compares the IMU angle estimations to the potentiometer reference system.

To justify the applicability of the IMU sensors in estimating knee joint angle during normal walking, we related the sensor error to the normal range of motion data from literature (68° flexion/extension, 10° abduction/adduction, and 13° internal/external rotation [17] by computing the percentage error. The observed errors of this specific IMU sensor system are 5% for flexion/extension, 34% abduction/adduction and 22% for internal/external rotation.

## 4. Discussion

The instrumented gimbal was developed to evaluate the performance of IMU sensors in estimating 3D joint angles. It simulates the full range of motion experienced by the knee joint while measuring anatomical joint angles independently from motion sequence. Consequently, it allows a direct comparison between the potentiometer readings to the 3D knee joint angle estimates from the IMUs, which was previously unavailable.

Our study is methodologically distinct from previous work quantifying 3D IMU error, which was done using human motion and a reference measurement system. However, by comparing our results with previous studies, the relative importance of the sources of error can be inferred. Favre et al. [12] reported RMSE angle errors of 8.1° in flexion/extension, 6.2° in abduction/adduction, and 4.0° in internal/external rotation, which are much higher than the 3.20°,3.42°, and 2.88° reported in this study. The smaller error magnitudes from our results are most likely due to three factors. First, we obtained accurate sensor attachment matrices with the use of IMU mounting brackets, essentially eliminating sensor attachment error introduced by the user, which is impossible in human studies. Second, we quantified the sensor accuracy by comparing the IMU angle estimates with those directly measured from the accurate gimbal device, which reduced the error potentially introduced by a secondary reference system such as the magnetic marker system. Third, by introducing a double calibration procedure, one before and one after data collection, we reduced the effects of earth frame alignment drift.

We observed inter-trail variability during this study and suspect the variability originated from two sources. First, this study could not directly quantify the relationship between angle estimation accuracy to motion frequency. All five trials were conducted such that maximum angular velocities were within the range of normal gait. However, the motion sequence was not controlled, which could introduce intra-trial variability [3,18,5]. Second, sensor drift introduced variability between trials as seen in Table 1. Because we can only estimate drift twice, before and after data collection, the best model predicting the drift during the experiment was a linear model. However, we observed that the drift did not follow a linear model exactly, and the degree of variation from the linear model was most likely different for each trial. Similar effects of drift on joint angle estimation error have been reported previously [10,18,9,19]. A model for accurately estimating sensor drift is desirable in order to reduce inter-trial variability.

One limitation of this study is the use of the proprietary orientation estimation algorithms provided by the sensor supplier. The accuracy results reported here only reflect the performance of this specific sensor and algorithm. However, we found that the sensor performance was within the manufacturers' specifications of 4° (two sensors × 2° per sensor), as shown by the RMSE results.

In summary, we have successfully quantified the IMU sensor error in estimating 3D joint angles, and found that the error is expected to be between 1.5° and 3.5° for motion of frequency similar to that of human gait. By comparing to previous work involving human subjects that report higher errors, we can deduce that a combination of sensor attachment, accuracy of reference systems, and estimation of earth frame drift also contributes considerably to the errors expected when working with inertial angle measurement. For the purposes of quantifying performance of different sensor systems and angle estimation algorithms, this instrumentation and methodology is recommended over the use of motion capture systems as a reference because the gimbal provides a highly accurate and reliable reference system for 3D motion. In addition, this setup can easily mimic different joint motion patterns and therefore, it could be used to verify experimental protocols and identify potential problems before human experimentation.

## Acknowledgment

We would like to gratefully acknowledge the support from NSERC discovery grants to QL, KD and NSERC USRA to AB.

## Conflict of interest

There is no conflict of interest involved with this study from any of the authors.

## References


[1] Rowe PJ, Myles CM, Walker C, Nutton R. Knee joint kinematics in gait and other functional activities measured using flexible electrogoniometry: how much knee motion is sufficient for normal daily life? Gait & Posture 2000;12(2):143–55.

[2] Li Q, Naing V, Donelan JM. Development of a biomechanical energy harvester. Journal of Neuroengineering and Rehabilitation 2009;6(1):22.

[3] Cooper G, Sheret Y, McMillian L, Siliverdis K, Sha N, Hodgins D, et al. Inertial sensor-based knee flexion/extension angle estimation. Journal of Biomechanics 2009;42(16):2678–85.

[4] Willemsen A, van Alsté J, Boom H. Real-time gait assessment utilizing a new way of accelerometry. Journal of Biomechanics 1990;23(8):859–63.

[5] Mayagoitia RE, Nene AV, Veltink PH. Accelerometer and rate gyroscope measurement of kinematics: an inexpensive alternative to optical motion analysis systems. Journal of Biomechanics 2002;35(4):537–42.

[6] Tong K, Granat MH. A practical gait analysis system using gyroscopes. Medical Engineering & Physics 1999;21(2):87–94.

[7] Dejnabadi H AK, Jolles BM. A new approach to accurate measurement of uniaxial joint angles based on a combination of accelerometers and gyroscopes. IEEE Transactions on Biomedical Engineering 2005;52(8):1478–84.

[8] Takeda R, Tadano S, Todoh M, Morikawa M, Nakayasu M, Yoshinari S. Gait analysis using gravitational acceleration measured by wearable sensors. Journal of Biomechanics 2009;42(3):223–33.

[9] Godwin A, Agnew M, Stevenson J. Accuracy of inertial motion sensors in static, quasistatic, and complex dynamic motion. Journal of Biomechanical Engineering 2009;131(11):114501–11.

[10] Brodie MA, Walmsley A, Page W. Dynamic accuracy of inertial measurement units during simple pendulum motion. Computer Methods in Biomechanics and Biomedical Engineering 2008;11(3):235–42.

[11] Favre J, Jolles BM, Aissaoui R, Aminiana K. Ambulatory measurement of 3D knee joint angle. Journal of Biomechanics 2008;41(5):1029–35.

[12] Favre J, Aissaoui R, Jolles BM, de Guise JA, Aminian K. Functional calibration procedure for 3D knee joint angle description using inertial sensors. Journal of Biomechanics 2009;43(14):2330–5.

[13] Grood E, Suntay W. A joint coordinate system for the clinical description of three-dimensional motions: application to the knee. Journal of Biomechanical Engineering 1983;105(2):136–45.

[14] Wu G, Cavanagh PR. Isb recommendations for standardization in the reporting of kinematic data. Journal of Biomechanics 1995;28(10):1257–61.

[15] Churchill D. Quantification of human knee kinematics using the 3dm-gx1 sensor, Tech Rep from Microstrain Inc. (2004).

[16] Bland J, Altman D. Statistical methods for assessing agreement between two methods of clinical measurement. The Lancet 1986;327(8476):307–10.

[17] Kavanagh J, Morrison S, James D, Barrett R. Reliability of segmental accelerations measured using a new wireless gait analysis system. Journal of Biomechanics 2006;39(15):2863–72.

[18] Saber-Sheikh K, Bryant E, Glazzard C, Hamel A, Lee R. Feasibility of using inertial sensors to assess human movement. Manual Therapy 2010;15(1):122–5.

[19] Luinge HJ, Veltink PH. Measuring orientation of human body segments using miniature gyroscopes and accelerometers. Medical & Biological Engineering & Computing 2005;43:273–82.